**České vysoké učení technické v Praze**
**Fakulta dopravní**

**Czech Technical University in Prague**
**Faculty of Transportation Sciences**

Ing. Zoltán Szabó, Ph.D.

**Měření pozice a orientace objektů v 3D prostoru pomocí kamer**

**Measuring the position and orientation of objects in 3D space using cameras**

# Summary

Technological advances in 3D imaging as well as hardware and software facilities have generated enormous growth in both theoretical and applied scientific applications, especially over the past ten years. New real time applications now available, which weren't just a few years ago, along with advanced camera systems, have become a normal part of everyday life. Camera systems are used in many fields: In industry for car crash tests and machine inspection; in biomechanics combined with EMG devices to analyze human movement, such as clinical gait; in sports for material research and athletic training analysis, etc.

In this lecture, multi-camera systems for 3D localization have been addressed as useful tools for research and clinical applications mainly in medical area. They always provide reliable and accurate position determination when there is a free line of sight between the object under observation (patient) and cameras. It is also minimally annoying for the patient when passive markers are used. Most disadvantages of camera-systems can be eliminated through a carefully designed environment where measurement is done.

The lecture summarizes fundamentals of projective geometry, the process of camera calibration necessary for further measurement used for measuring the position and orientation of objects in 3D space and furthermore for movement analysis. Practical use of camera systems (including the self-proposed and existing BradykAn system) for 3D localization in medical research have been presented. It is evident, that 3D localization using cameras require solving a number of sub-problems, beginning with the design and choice of used components, calibration, synchronization, marker detection in each frame, matching of markers from different views, tracking the markers in time, calculation of spatial coordinates, derivation of characteristic motion parameters and creation of applications for routine measurements.

# Souhrn

Technologický pokrok v 3D zobrazení, stejně jako hardwarové a softwarové možnosti, zejména za posledních deset let, přinesly obrovský nárůst teoretických a aplikovaných vědeckých aplikací. K dispozici jsou nové aplikace pracující v reálném čase, které před pár lety nebyly a spolu s pokročilými kamerovými systémy se staly běžnou součástí každodenního života. Kamerové systémy se používají v mnoha oblastech: v automobilovém průmyslu u nárazových zkoušek, strojových kontrol, v biomechanice v kombinaci s přístroji EMG pro analýzu lidského pohybu, jako je klinické vyšetření chůze, v oblasti sportu pro materiálový výzkum, analýzu pohybu při atletickém tréninku, atd.

Tato přednáška je věnovaná vícekamerovým systémům jako užitečným nástrojům pro 3D lokalizaci ve výzkumu a klinických aplikacích, zejména v oblasti medicíny. Kamerové systémy poskytují spolehlivé a přesné určení polohy, kdy je přímá viditelnost mezi zkoumaným objektem (pacientem) a kamerami. Použití pasivních značek je méně obtěžující pro pacienta. Většina nevýhod kamerových systémů navíc může být odstraněna pomocí pečlivě navrženého prostředí, ve kterém se měření provádí.

Přednáška shrnuje základy projektivní geometrie, proces kalibrace kamery potřebné pro měření polohy a orientace objektů v 3D prostoru a dále pro analýzu pohybu. Jsou prezentovaná praktická využití kamerových systémů (včetně vlastního navrženého systému BradykAn) pro 3D lokalizaci v lékařském výzkumu. Je zřejmé, že 3D lokalizace pomocí kamer vyžaduje řešení řady dílčích problémů, počínaje návrhem a výběrem použitých komponentů, kalibraci, synchronizaci, detekci značek v každém snímku, přiřazování značek z různých pohledů, sledování značek v čase, výpočet prostorových souřadnic, odvození charakteristických parametrů pohybu a vytváření aplikací pro rutinní měření.

# Contents

# 1  Introduction

## 1.1  Position-sensing techniques

There are four basic position-sensing techniques: (i) acoustic ranging, (ii) mechanical articulated arm, (iii) magnetic field sensor, and (iv) optical tracker. Acoustic sensors receive signals which are emitted by ultrasonic emitters and determine location via time-of-flight. Mechanical sensors determine position based on measurements of joint angles and kinematics of the device. Magnetic sensors measure electrical currents induced in three orthogonal coils when the receiver is moved within a magnetic field. Finally, optical tracker systems track the position of one or more markers and use geometric triangulation to determine the location of these markers.

In this lecture, we deal with optical tracking systems because they provide reliable and accurate position determination for different applications where there is always a free line of vision between markers and cameras. The object is monitored from a distance by one or several cameras, and markers, attached to the part of object being measured. Further, optical trackers do not involve any magnetic field for determination of position data, and therefore do not incur any deformation of data in the presence of metallic structures. Most disadvantages of optical tracking can be eliminated by carefully designing the environment of the system.

# 2  Camera model

This part of the lecture is devoted to a brief discussion of some basic three-dimensional (3D) graphics concepts and terminology based on pinhole camera model. It gives a geometric aspect of automated measurement of 3D world using 2D image information obtained by cameras.

The pinhole camera is the simplest imaging system for modeling cameras in the shape of a closed box with a small hole in one of the sides. Light with an image passes through this small hole and inverts a projected image on the opposite side of the box (see Figure 2.1).

*Fig. 2.1: The pinhole camera.*
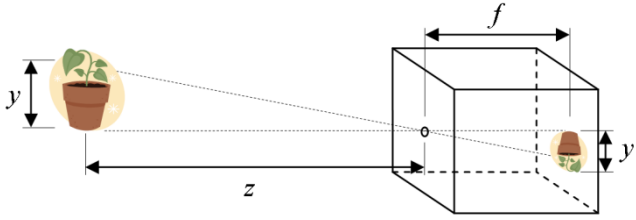
Let's introduce a coordinate system as in Figure 2.2. Let the origin of the coordinate system $c$ be located at the center of projection (the focal point), and let the $z$ axis coincide with the optical axis perpendicular to the image plane $\pi$. The distance from the focal point to the image plane is called focal length $f$. Similar triangles give

$$x' = -f\frac{x}{z} \text{ and } y' = -f\frac{y}{z}. \tag{2.1}$$
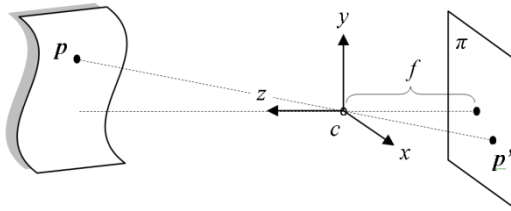


*Fig. 2.2: Pinhole imaging model. Perspective projection equations are derived from the collinearity of the point $p = (x, y, z)$ (on the object), its image $p' = (x', y')$ (on the image plane $\pi$) and the center of projection $c$ (origin of the coordinate system).*

Notice that there is a negative sign in formulae (2.1). This is because the image of an object appears to be upside down on the image plane. To eliminate this effect, we can simply flip the image $(x', y') \rightarrow (-x', -y')$. This corresponds to placing the image plane in front of the center of projection, making a frontal pinhole camera model, illustrated in Figure 2.3. In this case, the image of the point $p = (x, y, z)$ is given by

$$x' = f\frac{x}{z} \text{ and } y' = f\frac{y}{z}. \tag{2.2}$$
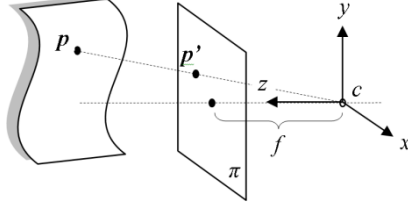
*Fig. 2.3: Frontal pinhole imaging model. The image plane $\pi$ is at the distance $f$ in front of the center of projection.*

In practice, the size of image plane $\pi$ is usually limited; hence not every point $p$ in space will generate an image $p'$ inside the image plane. The field of view limiting the image plane is defined as $\theta = 2arctan(r/f)$, where $r$ is the side of the image sensor (CCD)[1] and $f$ is the focal length.

Adopting the frontal pinhole camera model introduced above, we see that point $p$ represented by vector $\boldsymbol{p} = [x, y, z]^T$ is projected into the image plane at point $p'$ represented by vector $\boldsymbol{p}' = [x', y']^T$. Then equations (2.2) can be written in matrix form

$$\begin{bmatrix} x' \\ y' \end{bmatrix} = \frac{1}{z} \begin{bmatrix} f & 0 & 0 \\ 0 & f & 0 \end{bmatrix} \begin{bmatrix} x \\ y \\ z \end{bmatrix}. \tag{2.3}$$

This relationship using homogenous coordinates $\widetilde{\boldsymbol{p}} = [x, y, z, 1]^T$ and $\widetilde{\boldsymbol{p}'} = [x', y', 1]^T$, can be written as

$$\begin{bmatrix} x' \\ y' \\ 1 \end{bmatrix} = \frac{1}{z} \begin{bmatrix} f & 0 & 0 & 0 \\ 0 & f & 0 & 0 \\ 0 & 0 & 1 & 0 \end{bmatrix} \begin{bmatrix} x \\ y \\ z \\ 1 \end{bmatrix}. \tag{2.4}$$

The 3×4 matrix in equation (2.4) is called a camera matrix and can be decomposed into two matrices

$$\begin{bmatrix} f & 0 & 0 & 0 \\ 0 & f & 0 & 0 \\ 0 & 0 & 1 & 0 \end{bmatrix} = \begin{bmatrix} f & 0 & 0 \\ 0 & f & 0 \\ 0 & 0 & 1 \end{bmatrix} \begin{bmatrix} 1 & 0 & 0 & 0 \\ 0 & 1 & 0 & 0 \\ 0 & 0 & 1 & 0 \end{bmatrix} = K_f[I_{3\times3}|\boldsymbol{0}_{3\times1}]. \tag{2.5}$$

The second matrix $[I_{3\times3}|\boldsymbol{0}_{3\times1}]$ is often referred to as a standard or canonical projection matrix. The simplified expression of equation (2.4) is then

---

[1] In the case of flat image plane, the angle $\theta$ is always less than 180°.

$$z\widetilde{\boldsymbol{p}}' = K_f[I_{3\times3}|\mathbf{0}_{3\times1}]\widetilde{\boldsymbol{p}}. \tag{2.6}$$

Since the coordinate $z$ (depth of the point $p$) is usually unknown, we may simply write it as an arbitrary positive scalar $\lambda$

$$\lambda\widetilde{\boldsymbol{p}}' = K_f[I_{3\times3}|\mathbf{0}_{3\times1}]\widetilde{\boldsymbol{p}}. \tag{2.7}$$

Equation (2.7) expresses coordinates of point $p$ in the camera coordinate system introduced above. To continue, we will express point $p$ in a different coordinate system called the object coordinate system. Let superscript $c$ denote the camera coordinate system and similarly superscript $o$ the object coordinate system (see Figure 2.4).
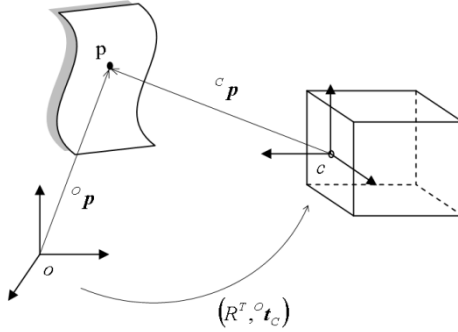


*Fig. 2.4: Using different coordinate systems for the camera and the object.*

If vector $^c\boldsymbol{p}$ refers to point p represented in coordinate system $c$, then the same point p is represented in object coordinate system $o$ by

$$^o\boldsymbol{p} = R^{T\,c}\boldsymbol{p} + {}^o\boldsymbol{t}_c, \tag{2.8}$$

where $R$ is a 3×3 rotation matrix that rotates coordinate system $o$ through at counterclockwise angles $\gamma$, $\beta$, and $\alpha$ to the position where its basis vectors are parallel with the basis vectors of the coordinating system $c$. Vector $^o\boldsymbol{t}_c$ represents the origin of the camera coordinate system with respect to the object coordinate system. Alternatively the vector $^c\boldsymbol{p}$ can be expressed as

$$^c\boldsymbol{p} = R(^o\boldsymbol{p} - {}^o\boldsymbol{t}_c). \tag{2.9}$$

Note: The rotation matrix is an orthonormal matrix, therefore, the inverse of a rotation matrix is its transpose ($R^{-1} = R^T$).

In block form using homogenous coordinates

$$\begin{bmatrix} {}^o\boldsymbol{p} \\ 1 \end{bmatrix} = \begin{bmatrix} R^T & {}^o\boldsymbol{t}_c \\ \boldsymbol{0}_{1\times3} & 1 \end{bmatrix} \begin{bmatrix} {}^c\boldsymbol{p} \\ 1 \end{bmatrix}, \tag{2.10}$$

Analogously, the vector ${}^o\boldsymbol{p}$ can be expressed in the camera coordinate system by the following transformation

$$\begin{bmatrix} {}^c\boldsymbol{p} \\ 1 \end{bmatrix} = \begin{bmatrix} R & -R^o\boldsymbol{t}_c \\ \boldsymbol{0}_{1\times3} & 1 \end{bmatrix} \begin{bmatrix} {}^o\boldsymbol{p} \\ 1 \end{bmatrix}, \tag{2.11}$$

$$\widetilde{{}^c\boldsymbol{p}} = H\widetilde{{}^o\boldsymbol{p}}, \tag{2.12}$$

where $H$ is referred as a homogeneous transformation matrix which contains what are known as camera extrinsic parameters which indicate external position and orientation of the camera in the 3D world (in our case with respect to the object coordinate system).

Based on knowledge of vector $\widetilde{{}^o\boldsymbol{p}}$ and homogeneous transformation matrix $H$, we can express vector $\widetilde{\boldsymbol{p}}'$ (representing the projection of point $p$ into the image plane) by substituting equation (2.12) into the equation (2.7), taking into account that $\widetilde{\boldsymbol{p}}$ in (2.7) is the same as $\widetilde{{}^c\boldsymbol{p}}$ in (2.12). An overall geometric model for an ideal camera can be described as:

$$\lambda\widetilde{\boldsymbol{p}}' = K_f[I_{3\times3}|\boldsymbol{0}_{3\times1}] \begin{bmatrix} R & -R^o\boldsymbol{t}_c \\ \boldsymbol{0}_{1\times3} & 1 \end{bmatrix} \widetilde{{}^o\boldsymbol{p}}. \tag{2.13}$$

With multiplication of the canonical projection matrix $[I_{3\times3}|\boldsymbol{0}_{3\times1}]$ and the homogeneous transformation matrix we can simplify the equation above

$$\lambda\widetilde{\boldsymbol{p}}' = \left[K_fR| - K_fR^o\boldsymbol{t}_c\right]\widetilde{{}^o\boldsymbol{p}} = M_P\widetilde{{}^o\boldsymbol{p}}, \tag{2.14}$$

where

$$\left[K_fR| - K_fR^o\boldsymbol{t}_c\right] = M_P \tag{2.15}$$

is what we call a projection or camera matrix. Then the simplified expression of the equation (2.14) is

$$\lambda\widetilde{\boldsymbol{p}}' = M_P\widetilde{{}^o\boldsymbol{p}}. \tag{2.16}$$

## 2.1 Intrinsic parameters of the camera

The ideal model of a camera defined by the equations above is specified relative to a particular position of the image plane, centered

at the optical axis. Projected points are in that case expressed in so called normalized coordinates, relative to the principal point $(o_x, o_y)$, where the optical axis intersects the image plane (see Figure 2.5). In practice, using for example a digital camera the positions of projected points are obtained in terms of pixels and the origin of the image coordinate system is typically in the upper-left corner of the image. In order to extend the ideal camera model (2.16) taking into account pixel coordinates, we need to specify the relationship between the coordinate system centered at the principal point and the pixel array with an origin at the corner of the image.

Let's first specify the units along the $x$ and $y$ axes. If the normalized coordinates $(x', y')$ are specified in terms of metric units (e.g. millimeters), and $(x_S, y_S)$ are scaled versions that correspond to co-ordinates of the pixel, then the relationship can be described by a scaling matrix

$$\begin{bmatrix} x_S \\ y_S \end{bmatrix} = \begin{bmatrix} S_x & 0 \\ 0 & S_y \end{bmatrix} \begin{bmatrix} x' \\ y' \end{bmatrix}, \tag{2.17}$$

that depends on the size of the pixel (in metric units) along the $x$ and $y$ directions (see Figure 2.5).
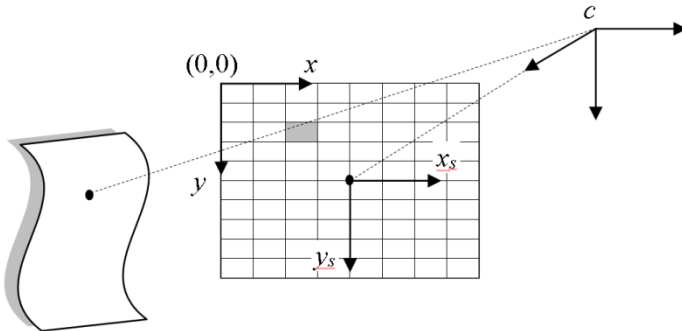


Fig. 2.5:  Transformation from normalized coordinates to coordinates in pixels.

When $S_x$ and $S_y$ are equal, each pixel is square, but in general, they can be different, and then pixels are rectangular. After scaling the normalized coordinates $(x', y')$, pixel coordinates $(x_S, y_S)$ are still specified relative to the principal point and may have a negative dimension, whereas pixel coordinates are conventionally specified relative to the upper-left corner. Therefore, we need to

translate the origin of the frame to the upper-left corner (see Figure 2.5)

$$x = x_S + o_x$$
$$y = y_S + o_y,$$
(2.18)

where $(o_x, o_y)$ are the coordinates of the principal point relative to the corner given also in pixels.

The above described steps (scaling and translation) can be connected together and can be written in a homogenous representation as

$$\begin{bmatrix} x \\ y \\ 1 \end{bmatrix} = \begin{bmatrix} S_x & 0 & o_x \\ 0 & S_y & o_y \\ 0 & 0 & 1 \end{bmatrix} \begin{bmatrix} x' \\ y' \\ 1 \end{bmatrix},$$
(2.19)

where $x$ and $y$ are again expressed in pixels. In this case, when pixel shape is not rectangular a more general form of transformation can be considered,

$$\begin{bmatrix} x \\ y \\ 1 \end{bmatrix} = \begin{bmatrix} S_x & S_\theta & o_x \\ 0 & S_y & o_y \\ 0 & 0 & 1 \end{bmatrix} \begin{bmatrix} x' \\ y' \\ 1 \end{bmatrix},$$
(2.20)

where $S_\theta$ is called skew factor and is proportional to $arctan(\theta)$, where $\theta$ is angle between the axes $x_S$ and $y_S$. Typically, the angle $\theta$ is very close to 90°, and hence $S_\theta$ is very close to zero.

The matrix is therefore

$$K_S = \begin{bmatrix} S_x & S_\theta & o_x \\ 0 & S_y & o_y \\ 0 & 0 & 1 \end{bmatrix},$$
(2.21)

then

$$\widetilde{\boldsymbol{p}_S} = K_S \widetilde{\boldsymbol{p}'}.$$
(2.22)

By combining the previous camera model (see equation 2.16) with the scaling and translation of the image coordinate system represented by matrix $K_S$, a more realistic model of transformation between a 3D point and its image can be obtained. A homogenous representation of the transformation is then

$$\lambda \widetilde{\boldsymbol{p}_S} = K_S M_P {}^o\widetilde{\boldsymbol{p}}.$$
(2.23)

$$\lambda \widetilde{\boldsymbol{p}_S} = [KR| - KR^o \boldsymbol{t}_c] {}^o\widetilde{\boldsymbol{p}},$$
(2.24)

where

$$K = K_S K_f = \begin{bmatrix} S_x & S_\theta & o_x \\ 0 & S_y & o_y \\ 0 & 0 & 1 \end{bmatrix} \begin{bmatrix} f & 0 & 0 \\ 0 & f & 0 \\ 0 & 0 & 1 \end{bmatrix} = \begin{bmatrix} fS_x & fS_\theta & o_x \\ 0 & fS_y & o_y \\ 0 & 0 & 1 \end{bmatrix} \quad (2.25)$$

is an upper triangular $3 \times 3$ matrix collecting all the parameters that are intrinsic to a particular camera, and is therefore called the intrinsic parameter matrix or calibration matrix of the camera. Then the projection or camera matrix (2.15) can be rewritten as

$$M = [KR| - KR^o \boldsymbol{t}_c], \quad (2.26)$$

including the intrinsic parameters of the camera, too. The projection equation will be

$$\lambda \widetilde{\boldsymbol{p}_S} = M \widetilde{{}^o\boldsymbol{p}}. \quad (2.27)$$

The process where intrinsic parameters of a camera (i.e. components of the calibration matrix $K$) are calculated is called camera calibration.

## 2.2 Image distortion

The pinhole camera model is an idealized representation for physical imaging systems, performing projective transformations between object points and image plane projections. For real applications this ideal situation will not hold, since it is very difficult or impossible to construct an optical system in which all lenses are perfectly parallel, with their optical centers perfectly aligned and their curvature meeting the required form. As a result, the deviations may be several pixels relative to the ideal model. For example, in Figure 2.7 the image has severe radial distortion. In practice image distortion can be expressed as a transformation of the pinhole projection estimation, mapping an ideal (distortion-free) image point defined by vector $\widetilde{\boldsymbol{p}_S}$ into a real distorted location $\widetilde{\boldsymbol{p}}_r$ (see Figure 2.6).
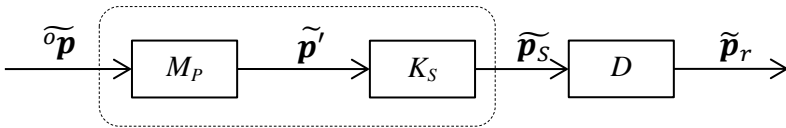


*Fig. 2.6: Schematic complete imaging system model including projection and distortion transformations.*

*Fig. 2.7: Radial distortion of the image.*

# 3 Multiply view geometry

In this lecture, we examine relations that arise when a single image is captured by two or more cameras. The geometric setting for two cameras – epipolar geometry - is illustrated in Figure 3.1. Note, that the geometry of multiple views may result from views acquired simultaneously as mentioned above, as in the case of stereo images, or from views acquired sequentially, for example by a single camera moving relative to the static image. These two situations are geometrically equivalent and will not be differentiated further.

The epipolar geometry is independent of the scene structure, and only dependent on the internal parameters of cameras and their relative position.
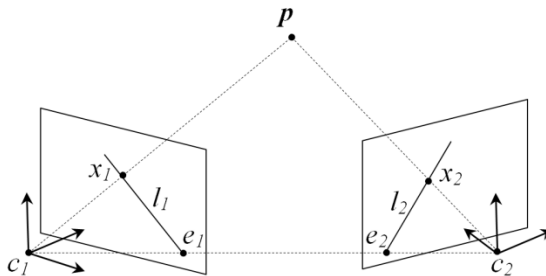


*Fig. 3.1: The geometry of two cameras showing the epipolar geometry.*

Suppose point $p$ in 3D space is imaged at $x_1$ in the first view and $x_2$ in the second view. As shown in Figure 3.1 image points $x_1$ and $x_2$, point $p$, and camera centers $c_1$ and $c_2$ are coplanar. We denote this plane by $\pi$ and call it the epipolar plane. The line joining the two camera centers is called the baseline.

Suppose now that we know $x_1$, and need to determine the corresponding point $x_2$ in the second image. The plane $\pi$ is unambiguously determined by the rays defined by $x_1$ and the baseline. Then, we need only search along the intercept of the epipolar plane $\pi$ and the second image plane for the corresponding point $x_2$. If we call this line of intercept the epipolar line (marked $l_2$ in Figure 3.1), we need only search along this line for the corresponding point $x_2$ (we reduce the dimensionality of the search space for correspondence between $x_1$ and $x_2$ from 2D to 1D).

## 3.1  Fundamental matrix

The fundamental matrix is an algebraic representation of epipolar geometry. It can be derived from the mapping between a point in one image to its corresponding epipolar line in the other image ($x_1 \rightarrow l_2$) in terms of the known projection matrices $M_1$ and $M_2$ of the left and right cameras. Moreover the fundamental matrix satisfies the condition that for any pair of corresponding points $x_1$ and $x_2$ in the two images

$$\widetilde{\boldsymbol{x}_2}^T F \widetilde{\boldsymbol{x}_1} = 0, \tag{3.1}$$

since $x_2$ lies on the epipolar line $l_2$, i.e. $\widetilde{\boldsymbol{x}_2}^T \widetilde{\boldsymbol{l}_2} = 0$.

The importance of the relation (3.1) is that it enables the fundamental matrix $F$ to be computed from image correspondences alone (without camera matrices). In general at least 7 correspondences are required to uniquely compute $F$ [9].

## 3.2  Camera calibration

Camera calibration is a process of determining intrinsic and extrinsic parameters of a camera. In many cases, overall performance of a camera system depends strongly on accuracy of calibration. Several methods are presented in the literature [2], [3], [4], [5], [7], [12] and basically they can be thought of as a two-stage process:

1. Estimating projection matrix $M$ that represents a complete viewing operation (2.26)

2. Estimating the intrinsic and extrinsic parameters from $M$. This stage may not be necessary in some applications, e.g. in the case of stereo vision.

There are two main approaches to estimating $M$, 1) with known and 2) with unknown scenes.

In the case of a known scene, a set of 3D points and corresponding 2D image points are used in order to define a linear equation system, which provides elements of $M$. The scene contains so called calibration objects or targets, whose shapes and dimensions are a priori known. This approach is also called as photogrammetric calibration.

The approach with an unknown scene does not require explicitly known calibration objects, but the correspondence between image points in different views must be established and intrinsic camera parameters would not change during calibration.
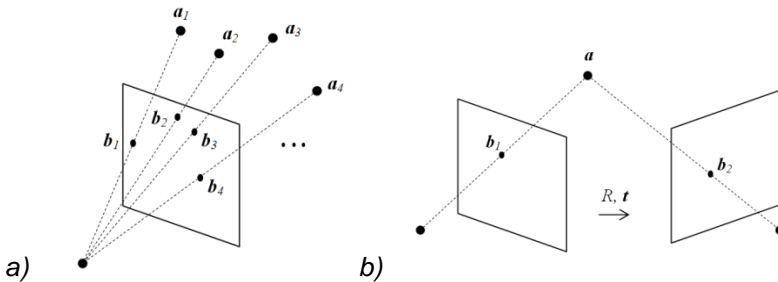


Fig. 3.2:  a) Camera calibration from a known scene; b) Camera calibration from an unknown scene.

## 3.3  Markers

Markers are attached to an object (e.g. human body) and, based on their positions the anatomical landmark points are determined.

Markers should keep their relative positions to anatomical landmark points constant during measurement. They should also be lightweight and minimally influence the analyzed object. In image-based analysis, markers must be seen by cameras otherwise their position cannot be determined.

We can basically distinguish two types of markers - active and passive. Active markers emit light. Their advantage is that identification is easy. The disadvantage is that active markers require an energy source.

Passive markers have the important advantage that they incur almost no discomfort for the human or animal, as they are lightweight and need no wired connection. The drawback of passive markers is that they need to be identified on each frame because relative positions of the markers may change as a result of displacement. When trajectories of two markers cross each other, further identification of each marker after crossing requires a priori knowledge of the studied movement.

The form of a marker must be selected so that its projection to the sensor plane has no effect to the accuracy of measurement. It follows that the shape of a marker should result in a circular projection. For 3D applications spherical shape is satisfactory.

## 3.4 Positional sensitivity of the optical system

Choosing a camera for an optical system determines only part of its capability. Geometric configuration of the cameras and the observed object also has a profound effect on the results. Positional sensitivity of the system is determined by angular resolution of the optical sensors due to the finite number of sensing elements, the distance between the investigated point on the observed object and the sensor, and on the geometric configuration of the optical sensors. Angular resolution is determined by the field of view of the sensor and resolution of measurements on the image plane.

For maximum accuracy, the cameras should be as distant as possible from each other and nearly at right angles to one another. Unfortunately placing the cameras too far apart may cause another problem because all the cameras must have a view of the investigated point in order to compute its 3D position.

# 4  3D measurements using cameras in practice

## 4.1 Bradykinesia analysis

Bradykinesia is the leading symptom in Parkinson´s disease (PD), crucial for diagnosis and for estimating functional disability of patients, and for which several clinical rating scales are used [6]. However, these rating scales are based on subjective evaluation expressed on an ordinal scale. Such evaluation fails not only to

cover severity nuances associated with bradykinesia, but also to monitor its progression in time. Therefore, a camera system BradykAn was developed in cooperation with the Department of Neurology and Clinical Neuroscience Centrum 1st Faculty of Medicine and General Teaching Hospital in Prague.

During the measurement, the 2D positions of the reflective markers are automatically found in the image sequences (from both cameras), and the 3D positions of markers are computed within a half millimeter of accuracy. The 3D movement of the markers (fingers) is subsequently processed and parameters characterizing given movements are computed (see Fig. 4.1).



1) Markers on the first knuckles of the forefinger and thumb

2) Subject performs finger tapping movements

3) The system records 3D trajectories of markers .

| | Average | Decrement |
|---|---|---|
| Amplitude | 8.45 cm | 13 % |
| Closing velocity | 85.21 cm/s | 8 % |
| Opening velocity | 50.20 cm/s | 5 % |
| Frequency | 2.45 Hz | 2 % |

5) Movement parameters are computed.

4) Distance of the markers is computed.
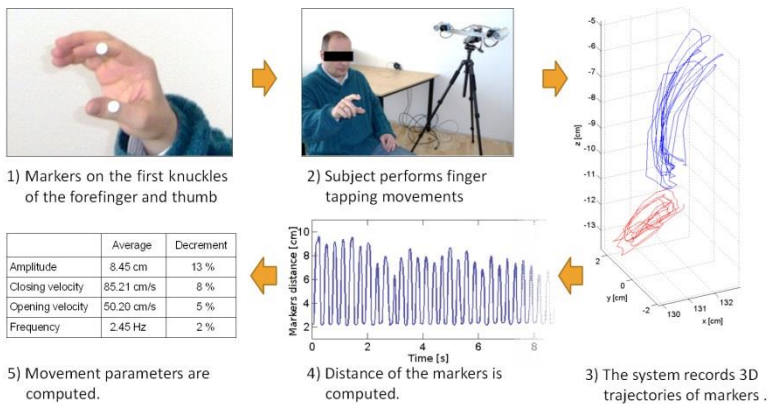
*Fig. 4.1: BradykAn: contactless 3D capture of finger tapping*

## 4.2 Gait analysis

Gait analysis is used to evaluate progress of patients and the effectiveness of their medical treatment. Patients show unusual patterns of gait because of physical deformities, irregular rotation of leg joints, and muscle tone issues.

Patients are measured with passive markers placed on the specific parts of the body. The coordinates of each marker are captured and a 3D model of each patient is created. Angle, velocity, cadence and other variables are derived from the data.

*Fig. 4.2: Specialized gait laboratory at the Department of Pediatric Orthopedics in Graz University Hospital (left) using Vicon motion capture system with ten cameras (right).*

## 4.3  Camera systems in automotive industry

Multi-camera systems offer significant advances in measurement capabilities for crash test facilities in the automotive industry. These systems are fast, and provide results that document all test results in accordance with regulatory requirements. In car crash tests, both movement and deformations on dummies and on the actual car parts need to be analyzed. Crash tests are taken under controlled conditions with markers applied to parts that are of interest. High-speed cameras are used to ensure an accurate record of fast movements (typically, 1000 frames/s or more is used). Cameras are used both off-board and on-board.



*Fig. 4.3:  Multi-camera measuring system for dynamic capture of engine movements or movements of any fixed bodies (left). Mounting frame for car reference points on engine block and vehicle (right) [1].*

# 5 Related and used literature

[1] Accurex, High-Accuracy 3-Dimensional Measurement Systems: [online], 10 2012. URL http://www.accurexmeasure.com/

[2] Faugeras, O., Luong, D., and Maybank, Q.: Camera selfcalibration: Theory and experiments. ECCV'92, Lecture notes in Computer Science, 588:321-334, 1992.

[3] Hartley, R.I.: Self-calibration from multiple views with a rotating camera. In Proc. European Conf. on Computer Vision, pages 471-478, Stockholm, Sweden, 1994.

[4] Hartley, R.I.: An algorithm for self calibration from several views. Proceedings of the IEEE Conf. on Computer Vision and Pattern Recognition, Seattle, WA, p 908–912, 1994.

[5] Heikkila, J.; Silven, O.: A four-step camera calibration procedure with implicit image correction. In Proc. IEEE Computer Society Conf Computer Vision and Pattern Recognition, 1997, pp. 1106–1112.

[6] Homann, C.; Suppan, K.; et al.: The bradykinesia akinesia incoordination test (BRAIN TEST(C)), an objective and user-friendly means to evaluate patients with parkinsonism. Movement Disorders, vol. 15, no. 4, 2000: pp. 641–647.

[7] Krupička, R., Szabó, Z., Vítečková, S., Kauler, J., Jiřina, M. - et al. Zařízení pro měření bradykineze pohybů prstů horní končetiny. Užitný vzor Úřad průmyslového vlastnictví, 23407. 2012-02-13. (in Czech)

[8] Pajdla, T.: Camera Calibration and Euclidean Reconstruction from Known Observer Translations. CVPR 1998, pp. 421-426, IEEE June 1998.

[9] Ruzicka, E., Krupicka , R., Zarubova , K., Szabo , Z., et al.: BradykAn: A New Reliable Tool For Measuring Bradykinesia. In MDS 17th International Congress of Parkinson's Disease and Movement Disorders, rocník 28, Sydney, Australia June 16-20, 2013.: Movement Disorders 2013, 6 2013.

[10] Sonka, M.; Hlavac, V.; Boyle, R.: Image Processing Analysis and Machine Vision. Thompson Learning, 2008.

[11] Szabó, Z., Štorková, B. Movement Analysis in Parkinson's Disease. Transactions on Engineering, Computing and Technology, ISSN 1305-5313, August 2006, vol. 14, pp. 18 - 21.

[12] Zhang, Z.: Camera calibration with one-dimensional objects. IEEE Trans. Pattern Analysis and Machine Intelligence, 26(7):892.899, 2004.

# Ing. Zoltán Szabó, Ph.D.

born on 27/07/1971 in Košice, Slovak Republic

## Education and training

- 2007 – 2008 Masaryk Institute of Advanced Studies, Czech Technical University in Prague, Course of Management. Thesis title: "Development of foreign relations on FBME CTU in Prague".
- 1994 – 2001 Department of Biomedical Engineering, Faculty of Electrical Engineering and Computer Science, Brno University of Technology, Czech Republic, Branch of study: Electronics and communication. Thesis title: "Contour Coding for Compression of Still Images and Image Sequences". Ph.D.
- 1998 – 1994 Department of Radioelectronics, Faculty of Electrical Engineering and Computer Science, Technical University Kosice, Slovakia, Diploma project title: "Spectral Analyser based on DSP56000 signal processor". Ing.

## Work experience

- 2004 – onwards, Assistant-Lecturer, Head of Department (2009 - onwards); Deputy head of Department (2007 – 2008), Department of Biomedical Informatics, Faculty of Biomedical Engineering, Czech Technical University in Prague
- 1994 – 2004, Assistant-Lecturer (2002 - 2004); Technical assistant (October 1994 – April 2002) Department of Biomedical Engineering, Faculty of Electrical Engineering and Computer Science, Brno University of Technology
- March 1996 – May 1996 and May 1997 – July 1997 Advanced research in microelectronics industry Researcher, Working in a research team dealing with contour image compression for MPEG-4 standard. IMEC, Leuven, Belgium

## Research achievements

Author or co-author of 2 journal papers with impact factors, 4 papers in reviewed international and 6 papers in national journals, more than 23 international and 15 national conference papers, 6 utility models

## Research projects

Principal investigator and co-investigator of more than 20 projects (IGA MZ, OP VK, GA ČR, AKTION, FRVŠ, SGS, ESF, CESNET)

## Selected publications

- KRUPIČKA, R., SZABÓ, Z., VÍTEČKOVÁ, S., RŮŽIČKA, E. *Motion Capture System for Finger Movement Measurement in Parkinson Disease,* Radioengineering journal - accepted paper for publishing 2014. ISSN 1210-2512. IF: 0.687 (2012)

- ŠVEHLÍK, M., KRAUS, T., STEINWENDER, G., ZWICK, E.B., LADECKÝ, M., SZABÓ, Z., LINHART, W.E. *Repeated multilevel Botulinum Toxin A treatment maintains the long-term walking ability in children with cerebral palsy*, Czech and Slovak Neurology and Neurosurgery, 2012, vol. 75, no. 6, p. 737-741, Print ISSN: 1210-7859, Online ISSN: 1802-4041. IF: 0.279 (2011)

- ČULÍK, J., SZABÓ, Z., KRUPIČKA, R. *Human Downfall Simulation*. In Recent Advances in Mechatronics 2008-2009. Berlin: Springer-Verlag, 2009, p. 437-442. ISBN 978-3-642-05021-3.

- SZABÓ, Z., ŠTORKOVÁ, B., HOZMAN, J., ZANCHI, V. *Objective Assessment of Patients with Parkinson's Disease.* In Proceedings of the 3rd WSEAS International Conference on Remote Sensing (REMOTE´07) - Chalenges in Remore Sensing. Athens: WSEAS Press, 2007, p. 39-42. ISBN 978-960-6766-17-6.

- SZABÓ, Z. *Analýza pohybu.* Biomedicínské inženýrství před námi. Praha: ARSCI, 2007, s. 53-59. ISBN 978-80-86078-83-0.

- SZABÓ, Z., ŠTORKOVÁ, B. *Movement Analysis in Parkinson's Disease*. Transactions on Engineering, Computing and Technology, ISSN 1305-5313, August 2006, vol. 14, s. 18 - 21.

- SZABÓ, Z., DEMJÉNOVÁ, E. *Multi-Camera System for Navigation in Medicine*. Acta Mechanica Slovaca, ISSN 1335-2393, 2005, roč. 2005, č. 2-A/2005, s. 325 - 330.

- SZABÓ, Z. *Graphical Representation of 1D and 2D Uniform and Non-uniform B-Splines*. International Transaction on Computer Science and Engineering, ISSN 1738-6438, 2005, roč. 2005, č. vol. 16, no. 1, s. 192 - 204.

- SZABÓ, Z. *Contour Image Data Compression Using Spline Wavelets*. Journal of Electrical Engineering, ISSN 1335-3632, 2004, roč. 55, č. 11-12, s. 290 - 584.

- KRUPIČKA, R., SZABÓ, Z., VÍTEČKOVÁ, S., KAULER, J., JIŘINA, M. - et al. *Zařízení pro měření bradykineze pohybů prstů horní končetiny.* Užitný vzor Úřad průmyslového vlastnictví, 23407. 2012-02-13.

- KAULER, J., SZABÓ, Z., HÁNA, K., SMRČKA, P. *Zařízení pro řízení kinematického řetězce pomocí svalů.* Užitný vzor Úřad průmyslového vlastnictví, 20180. 2009-11-03.